In situ Investigation of the Rheological and Dielectric Properties of a Cross-linking Carbon Nanotube-Thermosetting Epoxy

Journal:	*Soft Matter*
Manuscript ID	SM-ART-05-2023-000622.R2
Article Type:	Paper
Date Submitted by the Author:	20-Jul-2023
Complete List of Authors:	Ramos, Paolo; Northwestern University, Chemical and Biological Engineering Sarmah, Anubhav; Texas A&M University College Station, Chemical Engineering Green, Micah; Texas A&M University College Station, Chemical Engineering Richards, Jeffrey; Northwestern University, Chemical and Biological Engineering

SCHOLARONE™
Manuscripts

Title

In situ Investigation of the Rheological and Dielectric Properties of a Cross-linking Carbon

Nanotube-Thermosetting Epoxy

Author Names and Affiliations

Paolo Z. Ramos [a,‡] , E-mail: paoloramos2024@u.northwestern.edu

Anubhav Sarmah [b,‡], E-mail: anubhavsarmah@tamu.edu

Micah J. Green [b,c],*, E-mail: micah.green@tamu.edu

Jeffrey J. Richards [a],*, E-mail: jeffrey.richards@northwestern.edu

[a] *Department of Chemical and Biological Engineering, Northwestern University, Evanston,*

Illinois 60208, USA

[b] *Artie McFerrin Department of Chemical Engineering, Texas A&M University, College Station,*

Texas 77843, USA

[c] *Department of Materials Science and Engineering, Texas A&M University, College Station,*

TX, 77843, USA

[‡] Contributed equally to this work

* Corresponding authors

Abstract

Radio-frequency (RF) heating of thermosetting epoxies is an agile method to decouple the extrudability of epoxy resins from their buildability for additive manufacturing. Through this method, the resin is extruded in the liquid state at the early stages of curing. Then, an RF applicator induces a rapid and uniform increase in temperature of the resin, accelerating the solidification of the printed feature. Understanding the evolution of the resin's RF heating response as it cures is therefore critical in meeting the demands of additive manufacturing. In this work, we show that the high-frequency dielectric loss, determined using *in situ* rheo-dielectric measurements, of both neat and carbon nanotube (CNT) filled resins is correlated to the heating response at different temperatures throughout curing. Furthermore, we show that the presence of CNTs within the resin augments the heating response and that their dispersion quality is critical to achieving rapid heating rates during the cure.

Keywords

Carbon Nanotubes, Thermosetting Epoxy, Rheology of Curing, Electrochemical Impedance Spectroscopy, Radio-frequency Heating

Abbreviations

AC, alternating current; CNT, carbon nanotube; DIW, direct ink writing; EIS, electrochemical impedance spectroscopy; RF, radio-frequency; UV-vis, ultraviolet-visible

1. Introduction

Thermosetting epoxy resins are high-performance materials which have excellent mechanical strength, resistance to chemical degradation, and high thermal stability as a result of their permanent chemical cross-links.[1-4] The ability to reinforce these resins with nanoscale fillers to further enhance their mechanical, electrical, and thermal properties is particularly appealing for manufacturing high performance parts such as energy storage devices, piezoelectric sensors, aerospace and automotive industry parts, and drone rotor blades, among many more.[5-9] Direct Ink Writing (DIW) allows for free-form additive manufacturing of these materials, enabling rapid custom part manufacturing without the requirement of shape-specific molds.[10-12] However, the uncured resin ink tends to collapse if the printed structure goes beyond its yield stress during the print process, or the printed part collapses during the cure process due to a reduction of viscosity at higher temperatures.[13-15] These challenges make it difficult to decouple the printability of the resin from its mechanical properties post printing.[15-17] One possible solution to tackle this challenge is to accelerate the curing reaction and rapidly cure the extruded layer after deposition before printing the subsequent layers; this provides structural strength to the printed layers, thus allowing for shape retention and prevention of the collapse of the structure.[18,19]

Radio-frequency (RF) heating addresses this challenge by providing a direct and rapid temperature change necessary for DIW and additive manufacturing.[12,20-22] The responsiveness of a material to an RF field depends sensitively on the high frequency dielectric loss of the material, which is often too low in neat resins to induce rapid solidification.[23,24] However, this response can be enhanced by the addition of multi-walled carbon nanotubes (CNTs); CNTs increase the high frequency dielectric loss of the resin because they enhance its conductivity via electron transport.[25-28] This enhancement depends sensitively on the dispersion state of the CNTs, which can evolve as

the resin cures. Understanding the evolution of dielectric properties of CNT-filled resins is extremely relevant to predicting optimal curing conditions.[12,29-31] Therefore, there is a critical need to investigate the evolution of the dielectric properties during the cure of CNT-filled thermosetting epoxy resins and how they influence the heating rate of the material for RF curing.

In this work, we use rheo-dielectric measurements to investigate the evolution of the dielectric properties of neat and CNT-filled resins during the curing process as a function of curing temperature. We confirm that the dielectric loss is enhanced in the presence of CNTs. This enhancement, however, is diminished with decreasing curing temperature. This phenomenon results from the higher degree of agglomeration at lower temperatures caused by the slower curing kinetics. Finally, a correlation is established between the high frequency dielectric loss (determined at 1 MHz in our experiments) and the heating rate measured by resins subjected to an RF field. Our results show that dielectric measurements provide a quantitative probe of the responsiveness of a resin to an RF field, which can be used to engineer resin properties for DIW applications.

2. Experimental Methods

2.1. Sample Preparation

EPON 828 (ρ = 1.16 g/cm^3), a difunctional Bisphenol-A derived epoxide, was obtained from Hexion Incorporated (Columbus, OH). Jeffamine T403 (ρ = 0.98 g/cm^3), a trifunctional primary amine curing agent, was supplied by Huntsman Corporation (The Woodlands, TX). Multi-walled CNTs (ρ = 2.10 g/cm^3) were purchased from Cheap Tubes Incorporated (Grafton, VT). For samples with CNT fillers, 4 wt % of CNTs were uniformly dispersed in the epoxide using a planetary mixer for 10 minutes. The two-part thermosetting epoxy resin were prepared at a

1.00:0.49 wt/wt ratio of the epoxide and the curing agent for all samples (stoichiometrically balanced).[1,12,21]

2.2. Rheology

Small amplitude oscillatory shear experiments were performed using a TA instruments ARES G2 strain-controlled rheometer equipped with a custom-built, disposable plate-plate geometry (aluminum, 25 mm diameter). All measurements were taken with a gap of 0.2 mm, zeroed at the cure temperature. The temperature was controlled using a forced convection oven. Prior to combining the epoxide and the curing agent, the plate-plate geometry was pre-heated to and kept at the desired cure temperature for about 10 min. The resin was then uniformly mixed and rapidly loaded onto the geometry. Measurements were commenced immediately after returning to the set gap and cure temperature. The moduli of the samples were recorded as a function of time at 1 Hz with a strain amplitude of 0.1% (determined to be in the linear viscoelastic region from previously published work).[1]

2.3. Characterization

An Olympus BX51 Optical Microscope with 10X objective was used to observe the agglomeration of CNTs in an epoxy system as a function of curing time. Images were taken every 3 hours. UV-vis spectroscopy measurements were taken using a Shimadzu UV-vis 2500 to determine the dispersion stability of the CNT-epoxy system as a function of curing time. The wavelength was varied from 300 to 800 nm. Absorbance readings were taken until the sample was completely cured.

2.4. Electrochemical Impedance Spectroscopy

The impedance of the samples was probed using dielectric spectroscopy with a Keysight E4990A Impedance Analyzer. A 0.5 V alternating current (AC) electric field was applied to the

material at a frequency, f, range of 20 Hz to 5 MHz. The measured impedance was corrected for the residual impedance of the instrument and stray admittance of the open circuit using standard corrections. The permittivity, ε^*, was calculated from the corrected impedance, Z^*, following the equation $\varepsilon^* = C/(Z^* \varepsilon_0 i\omega)$ where C is the geometry cell constant of 1.02 m^{-1}, ε_0 is the vacuum permittivity, i is the imaginary unit, and ω is the angular frequency given as $\omega = 2\pi f$.

2.5. Radio-Frequency Heating

A Rigol DSG815 signal generator combined with a PRANA GN 500 power amplifier was used to generate RF waves. A stationary, coplanar applicator with a field length of 4 mm was used to apply the RF field, and the sample to be tested was exposed to this field for 3 s at 3 W power at a frequency of 130 MHz. A FLIR infrared thermal camera (FLIR Systems Inc., A655sc) was used to capture temperature as a function of time, and the initial heating rate for each run was calculated by measuring the slope of the temporal plot.

3. Results and Discussion

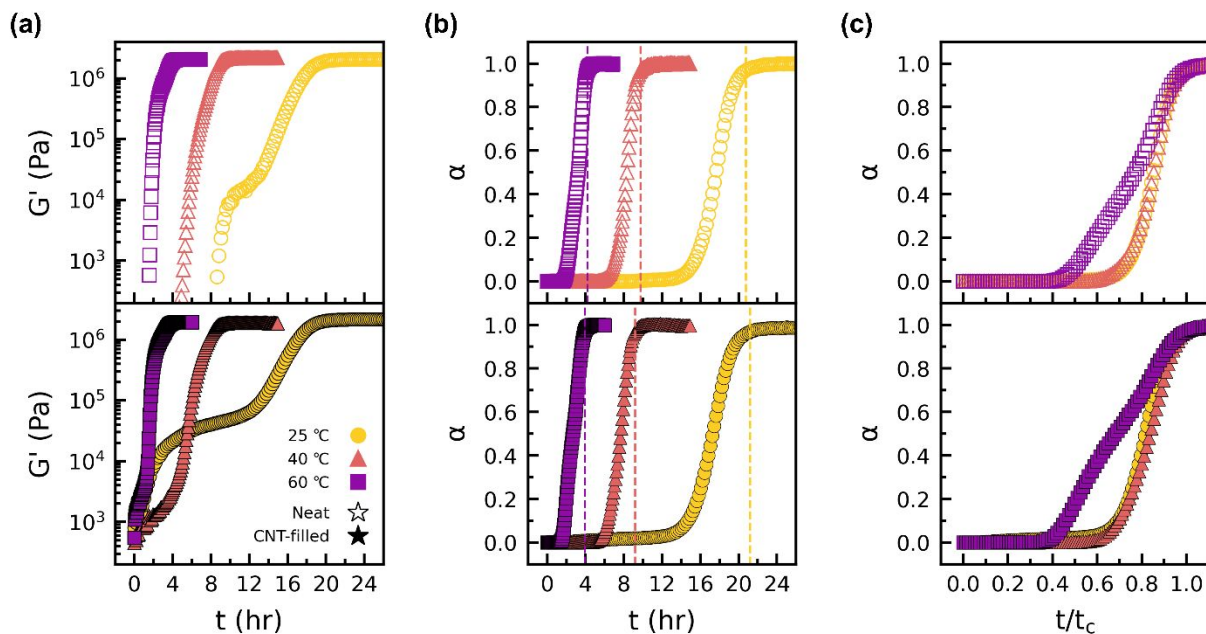## 3.1. Mechanical Behavior and Cure Times

Figure 1. (a) Time evolution (t) of the storage modulus (G') for the neat and CNT-filled resins at specified cure temperatures. Legend shown in the bottom panel applies to all subfigures. (b) The degree of conversion (α) calculated from G' as a function of time. The vertical, dashed lines represent the cure times (t_c) for each sample. (c) The degree of conversion replotted against time normalized to the determined cure times.

The rheological behavior of the epoxy resins was examined at different cure temperatures of 25, 40, and 60 °C. **Figure 1a** shows the time evolution of the storage modulus, G', during isothermal curing of the neat and 4 wt% CNT-filled resins. Three regions are typically present during the cure period: an initial, kinetic, and post period.[1] During the initial period, G' increases slightly with the formation of small, branched polymer chains. For the neat resins, G' could not be measured in the initial period, signifying a liquid-like behavior. On the other hand, the presence of CNTs elevates the starting values of G' to above 100 Pa. As seen in **Figure S1**, this led to values of tan(δ) smaller than 1, indicating that the CNTs have formed an elastic network.[32,33] For the CNT-filled sample cured at 25°C, G' rises steadily to about 60 kPa over the first 12 hours. This rheological feature, absent from the other samples, is indicative of a microstructural evolution of the CNT network. In the kinetic period, polymer chains link to form stress bearing networks and G' rises exponentially. All samples show a transition to the kinetic period at earlier times with

7

increasing cure temperatures, consistent with accelerated reaction kinetics.[1] Finally, G' plateaus to a constant value post cure as the maximum cross-link density is reached. The plateau modulus, G' (∞), was taken as the average of G' for the last ten seconds of each experiment and recorded in **Table 1**. These results are consistent with the expected range of moduli values from previously conducted rheology experiments on this system.[1] The addition of CNTs shows little reinforcement on $G'(\infty)$, with percent changes of +6.3, -13.3, and -4.9 with increasing cure temperature. CNTs are known to provide reinforcement[17,18] to thermosetting epoxy resin networks, but only when interfacial bonding occurs between CNTs and the epoxy matrix.[34] As the CNTs in this study are not surface modified, we do not anticipate strong interfacial bonding.

It is evident that the cure times of the resins decrease with increasing temperature due to the faster reaction kinetics. The rheological degree of cure, α, was calculated using the following equation:

$$\alpha = \frac{G'(t) - G'(0)}{G'(\infty) - G(0)} , (1)$$

where $G'(0)$ and $G'(t)$ is the storage modulus at the beginning and during the cure, respectively.[35] While G' does not track crosslinking of the molecular system as well as spectroscopic measurements,[36] α sufficiently estimates the depletion of reactive groups and captures the formation of the cross-linked network in our resin system. **Figure 1b** shows the plot of α over time for all samples (values of G' for the neat resins prior to the kinetic period, where measurements could not be resolved due to the torque resolution of the rheometer, were set to 0 Pa in the

Table 1. Determined plateau modulus and time of cure and of the thermosetting epoxy resins

calculations). An abrupt increase in α occurs in a time frame similar to that of the peak in tan(δ) for the CNT-filled resins in **Figure S1**. This is appropriate because the tan(δ) peak signifies the onset of the kinetic period.[37,38] Both the neat and CNT-filled resins at the same cure temperatures

begin the kinetic period approximately at the same time. The cure time, t_c, can be taken as the time required to attain $G'(\infty)$. Here, we approximated t_c as the time when α exceeds a threshold value of 0.97. As recorded in **Table 1**, the presence of CNTs had a negligible influence on t_c at all temperatures tested.

	25 °C		40 °C		60 °C	
	$G'(\infty)$ (GPa)	t_c (hr)	$G'(\infty)$ (GPa)	t_c (hr)	$G'(\infty)$ (GPa)	t_c (hr)
Neat	2.07	20.74	2.17	9.75	2.05	4.20
CNT-filled	2.20	21.19	1.89	9.16	1.95	3.93

To better assess the curing profile of the neat and CNT-filled resins, α was replotted in **Figure 1c** versus time normalized to t_c for each sample. Here the differences in the time evolution of the thermosetting epoxy resins are evident. Neat and CNT-filled samples cured at of 25 and 40 °C show near similar profiles, with the transition to the kinetic period at about $t/t_c = 0.6$ with the sudden upturn in α. The samples cured at the highest temperature of 60 °C, however, show the same transition occurring earlier around $t/t_c = 0.4$. The reduction in the transition time at 60 °C suggests an enhancement of the resin reaction kinetics. This may be attributed to the sample viscosity that decreases with increasing temperature, which would improve monomer diffusion.

3.2. Carbon Nanotube Microstructure

As demonstrated in the rheological measurements, the microstructure of CNTs undergoes a transient evolution during the cure. To investigate this further, optical microscopy image of the CNT-filled samples were taken to assess the initial and final state of the CNTs. **Figure 2** gives a visual representation of the dispersion quality of the CNT-epoxy system for each cure temperature.
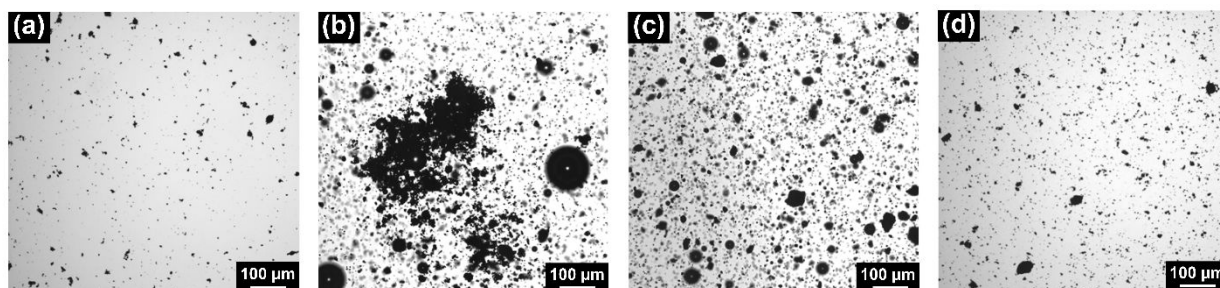

Figure 2. Optical microscopy images of 4 wt% CNT-filled resins (a) immediately after mixing the epoxy with the curing agent ($t/t_c = 0$) and cured ($t/t_c \geq 1$) at (b) 25, (c) 40, and (d) 60 °C.

At $t/t_c = 0$, the CNTs remain finely dispersed with only a small number of agglomerates discernable throughout the sample. At the end of cure, larger CNT agglomerates are present whose number and size depend on the cure temperature. With increasing cure temperatures, the extent of CNT agglomeration becomes less prominent. This is consistent with the faster curing kinetics that reduce the time for CNTs to agglomerate, thus maintaining their dispersion in the epoxy.[34] Additionally, the observation of massive agglomerates at the cure temperature of 25 °C is consistent with the enhancement of G' at early times observed in the rheology measurements. In contrast, higher cure temperatures of 40 °C and 60 °C suppresses this rheological feature because the curing time reduces substantially such that CNT agglomeration was inhibited.

To characterize the transient evolution of the CNT microstructure throughout the curing period, UV-vis spectroscopy was performed on the CNT-filled samples. The complete UV-vis spectra from a wavelength of 300 to 800 nm are shown in **Figure S2**, while **Figure 3** shows the absorbance of the system at 400 nm. For all curing temperatures, the absorbance initially decreases for short times, $t/t_c < 0.4$. The reduction in absorbance is more substantial for the sample cured at 25 °C, consistent with the results of **Figure 2** which shows that agglomeration of CNTs cured at 25 °C is highest. At longer times of $t/t_c > 0.4$, a gradual rise in absorbance occurs for all samples. We attribute this to the growth of progressively larger chains of reacted epoxide groups and the
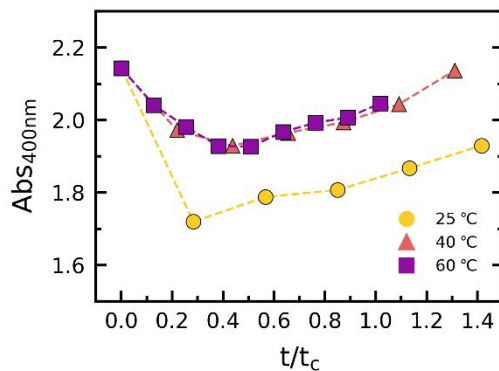

Figure 3. UV-vis absorbance taken at a wavelength of 400 nm (Abs_{400nm}) of the CNT-filled resins as a function of the normalized curing time (t/t_c).

formation of the epoxy network that increases the viscosity and absorbance of the sample. The overall trend of the UV-vis absorbance suggests that the CNTs predominantly agglomerate in the kinetic period where movement of the CNTs is yet to be inhibited by the cross-linking process. It is interesting to note that the absorbance of the CNT-filled resin continues to rise above $t/t_c = 1.0$. This would indicate that the curing process continues even though the rheological behavior has stopped changing.

3.3. High-frequency Electrical Conductivity

The addition of CNTs, their agglomeration, and the formation of the epoxy network will all have an effect on the material's dielectric properties. To assess this, we performed rheo-dielectric measurements on the samples during the curing process using a custom-built, demountable plate rheometer geometry pictured in **Figure S3**. For each sample and at each cure condition, the dielectric properties were monitored simultaneously with the storage modulus shown in **Figure 1**. The frequency dependent AC conductivity of the neat and CNT-filled resin at $t/t_c = 0$, 0.25, 0.5, and 1.0 is shown in **Figure S4**. Based on the measurements, the dielectric response of both the neat and CNT-filled resins are consistent with that commonly seen in literature.[39,40,41]

Understanding the impacts of the curing process on the high-frequency conductivity of the neat and CNT-filled resins is crucial in assessing their response to RF fields. The conductivity of the resins was measured at 1 MHz as a function of time. This frequency was chosen because it is within the relevant range for RF heating and is the highest resolvable frequency for our impedance analyzer. As shown in **Figure 4a**, the addition of CNTs to the neat resins leads to higher conductivities regardless of the cure temperature and degree of cure. This is a result of electronic conduction within the percolated CNT network.[41] In both the neat and CNT-filled samples, a peak
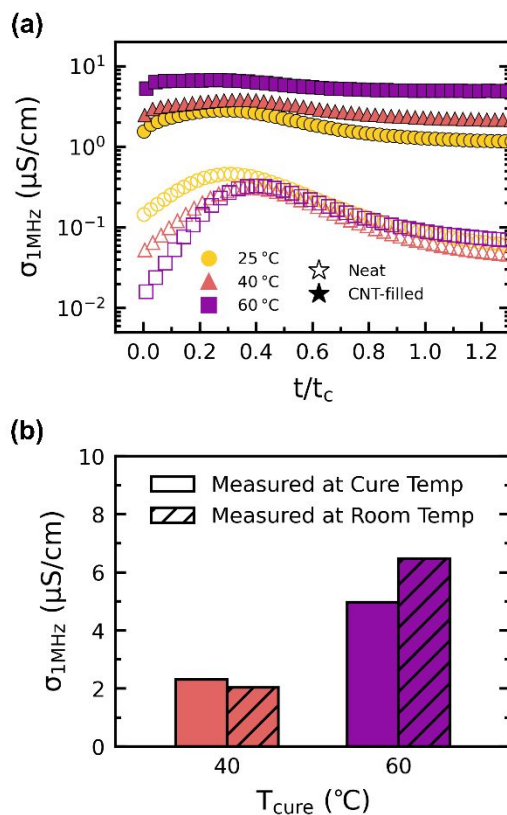
(a)

(b)

Figure 4. (a) Time evolution (t/t_c) of the conductivity at 1 MHz (σ_{1MHz}) of the neat and CNT-filled resins. (b) Conductivity at 1 MHz of the fully cured CNT-filled resins measured at cure and room temperature.

occurs in the conductivity around $t/t_c = 0.3$. This is similar to what has been observed in previous literature[28] and may be connected to the formation of the epoxy network. Indeed, as the curing reaction progresses past this point, the conductivity steadily decreases as the samples fully solidify. Fully cured samples show a minimum conductivity, consistent with the reduction of polarizability of the epoxide groups because of cross-linking. Additionally, the conductivities still decrease past $t/t_c = 1.0$, consistent with the continual increase of the UV-vis absorbance measurements of **Figure 3**. This reinforces the argument that the epoxy continues to react beyond what is rheologically measurable. Nevertheless, the enhanced conductivity of the CNT-filled samples is retained even at full cure, and the slow decrease in conductivity observed in the neat samples is significantly diminished beyond $t/t_c = 0.6$.

A large difference in the conductivity of the CNT-filled sample is observed as a function of cure temperature. While conduction in CNT-filled resins is known to be temperature sensitive, this variance can also be exhibited by the different CNT microstructure.[42] To deconvolute this contribution, the conductivity of the CNT-filled resins cured at 40 °C and 60 °C was remeasured at 25 °C. **Figure 4b** shows the comparison of the conductivity at cure temperature to that at 25 °C. It is evident that the temperature dependence of the conductivity alone cannot account for the variation between the two samples. We conclude that the large differences in the conductivity between CNT-filled samples is primarily due to the higher degrees of CNT dispersion.

3.4. Heating Rate Response

To evaluate how the effects of curing and CNT agglomeration impact the responsiveness of the samples to an RF field, we measured the temperature rise of the samples with time at a fixed RF field strength. To do this, a coplanar applicator shown in **Figure 5a** was used to generate fringing RF fields using a frequency of 130 MHz, the optimum heating frequency for this applicator. The resulting rise in temperature with time is plotted in **Figure S5** for both the neat and CNT-filled resins, all showed a linear increase with time. The heating rate was observed at multiple time points throughout the curing cycle and the heating rate determined at each experimental condition is summarized in **Figure 5b**.

The neat samples have an initial heating rate of ~4 °C/s that lowers to <1 °C/s at the end of cure, indicating strong inhibition of the polarizable epoxy and amine ends as the curing reaction progresses. The neat samples also show the same curing rate at equivalent values of t/t_c, which demonstrates that the rheological measurements provided an accurate basis for defining t_c. For the CNT-filled resins, the initial heating rate at $t_c = 0$ was ~8 °C/s, which is significantly higher than that of the neat resins. However, the heating rate of CNT-filled resins at different times across the
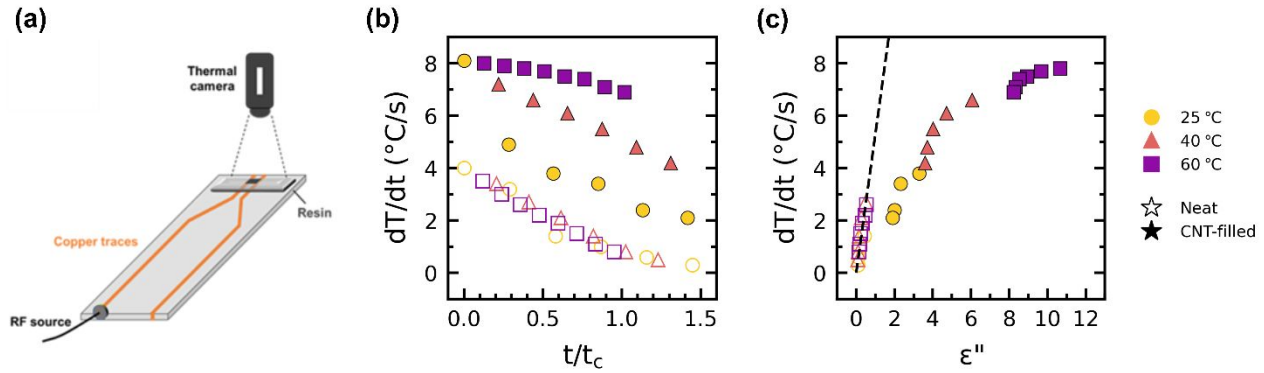
Figure 5. (a) Coplanar radio-frequency field applicator used to generate RF fields and heat up the resin. Temperature monitored using a thermal camera. (b) Time evolution (t/t_c) of the instantaneous heating rate (dT/dt) of the neat and CNT-filled resins when exposed to RF fields. (c) Correlation of the heating rate to the dielectric loss (ε'') of the resins for $t/t_c \geq 0.4$. Black, dashed lines are fits to the neat resin data according to Equation 2.

curing period varied based on the curing temperature as a function of t/t_c. The sample cured at 25 °C showed a decrease in heating rate similar in magnitude to the neat resins, albeit with an enhanced overall heating rate throughout the cure. As the curing temperature increased, the rate of decline of the heating rate with increasing cure time diminished. This observation is consistent with the improved dispersion quality of CNTs at higher curing temperatures (**Figure 2 and 3**), which leads to higher overall conductivity throughout the cure in the CNT-filled samples in **Figure 4**. The observation of decreased RF heating rate of the resin as it cures is consistent with the reduced conductivity of the resin as the curing reaction progresses.

We have established in our previous work that responsiveness of epoxies to RF fields depends on the electrical conductivity of the material.[23] A microscopic energy balance predicts a heating rate, $\frac{dT}{dt}$, that scales with the dielectric loss, ε'', of the material at the frequency of the RF field according to Equation (2):

$$\frac{dT}{dt} = \frac{E^2 \omega \varepsilon_0}{\rho \hat{C}_p} \varepsilon'' = C \varepsilon'', (2)$$

where ω is the RF frequency, E is the applied RF field strength, ρ is the material density, $\hat{C}_p$ is the material specific heat capacity, and ε_0 is the vacuum permittivity. For quantitative comparison, we

approximate ε'' in Equation 2 as $\varepsilon'' = \frac{\sigma_{1MHz}}{\omega\varepsilon_0}$. **Figure 5c** shows the heating rate as a function of ε'' for cure times of $t/t_c \geq 0.4$, when the resin system begins to undergo rapid changes in rheological and dielectric properties. In this scaled representation, a strong and linear correlation between the $\frac{dT}{dt}$ and ε'' is evident and is indicated by the dashed line. Additionally, the linear relationship indicates that dielectric heating is the dominant heating mechanism for the neat resins. The resulting slope C was used to calculate the effective RF field strength and found to be 28 kV/m consistent with finite element simulations of similar RF-field applicators.[31] In contrast, the CNT-filled samples exhibit a sub-linear relationship of $\frac{dT}{dt}$ and ε'' resulting in diminished responsiveness of the material to the RF field despite the higher dielectric loss. This indicates that enhanced dielectric loss that results from electrical conduction within the CNT network does not contribute linearly to the observed heating rate. Nonetheless, the higher dielectric loss CNT-filled samples had the highest rates observed, pointing to the important role that the dispersion quality of the CNTs plays in determining the responsiveness.

4. Conclusions

In summary, we studied the rheological behavior of a thermosetting epoxy resin with and without the addition of CNTs as the resin cross-links. For the tested cure temperatures of 25, 40, and 60 °C, differences in the rheological profile of the storage modulus signified a transient evolution of the CNT microstructure. Optical microscopy images of the cured samples confirmed agglomeration of the CNTs, with the degree of agglomeration decreasing with increasing cure temperature given faster curing kinetics. UV-vis spectroscopy demonstrated that CNT agglomeration occurred mostly before the formation of the cross-linked network, in which thereafter movement of the CNT within the system was inhibited. We further probed the effects of the CNT microstructure on the dielectric properties and RF field responsiveness of the samples.

CNT-filled resins showed greater enhancement in both the conductivity and heating rate with higher degrees of CNT dispersion. Finally, we correlated the dielectric loss of the resins to that of its heating rate at identical cure times past the onset of cross-linking. The CNT-filled resin has a higher dielectric loss compared to its neat counterpart; however, the heating rate of the CNT-filled resin rises sub-linearly with increase in dielectric loss.

The higher magnitude of heating rate observed in CNT-filled resin compared to the neat resin allows for rapid, volumetric heating, which is highly important for DIW and additive manufacturing applications with a layer-by-layer curing methodology. However, the sub-linear relationship observed in our measurements between the heating rate and the dielectric loss of the CNT-filled resins presents a diminished response of the CNTs to an RF field. We believe that the CNTs not only contribute to the dielectric loss of the resin but can also cause reflection of RF fields at high loadings. Careful consideration of the CNT loading and surface functionalization methods, which in turn may augment the mechanical properties of the resins, may help prevent this diminished relationship between heating rate and dielectric loss in CNT-filled resins. Nonetheless, *in situ* dielectric spectroscopy is a vaulable tool to determine the RF field responsiveness of a curing thermosetting epoxy resin. Further study into the tradeoff between the shielding effect and conductivity enhancement provided by the CNTs is needed to design time and energy efficient methodologies for RF curing.

Author Contributions

P.R. and A.S. contributed equally to this work. P.R. and A.S. performed the experiments, analyzed the data, and wrote the original draft. M.G. and J.R. supervised the work. All authors discussed the results and have given approval to the final version of the manuscript.

Conflicts of Interests

Jeffrey John Richards reports financial support was provided by National Science Foundation.

Table of Content Text

Monitoring the dielectric properties of a thermosetting resin allows for better understanding of how these materials respond to radio-frequency fields as the cure evolves, with possible applications in additive manufacturing.

Notes and References

1.   G. B. Tezel, A. Sarmah, S. Desai, A. Vashisth, M. J. Green. Kinetics of carbon nanotube-loaded epoxy curing: Rheometry, differential scanning calorimetry, and radio frequency heating. *Carbon.* **2021**;175:1-10.

2.   J. C. Domínguez. Chapter 4 - Rheology and curing process of thermosets. In: Guo Q, ed. *Thermosets (Second Edition).* Elsevier; 2018:115-146.

3.   B. Bilyeu, W. Brostow, K. P. J. J. o. M. E. Menard. Epoxy thermosets and their applications I: chemical structures and applications. **1999**;21(5/6):281-286.

4.   W. Johannisson, D. Zenkert, G. J. M. M. Lindbergh. Model of a structural battery and its potential for system level mass savings. **2019**;2(3):035002.

5.   H. J. Kim, Y. J. Kim. High performance flexible piezoelectric pressure sensor based on CNTs-doped 0–3 ceramic-epoxy nanocomposites. *Materials & Design.* **2018**;151:133-140.

6.   L. Mishnaevsky, K. Branner, H. N. Petersen, J. Beauson, M. McGugan, B. F. Sørensen. Materials for Wind Turbine Blades: An Overview. **2017**;10(11):1285.

7.   S. Rana, R. Alagirusamy, M. Joshi. A Review on Carbon Epoxy Nanocomposites. **2009**;28(4):461-487.

8.   P. Pissis. *Thermoset nanocomposites for engineering applications.* iSmithers Rapra Publishing; 2007.

9.   N. Mohd Nurazzi, M. R. M. Asyraf, A. Khalina, N. Abdullah, F. A. Sabaruddin, S. H. Kamarudin, S. b. Ahmad, A. M. Mahat, C. L. Lee, H. A. Aisyah, M. N. F. Norrrahim, R. A. Ilyas, M. M. Harussani, M. R. Ishak, S. M. Sapuan. Fabrication, Functionalization, and Application of Carbon Nanotube-Reinforced Polymer Composite: An Overview. *Polymers-Basel.* **2021**;13(7):1047.

10.   N. S. Hmeidat, D. S. Elkins, H. R. Peter, V. Kumar, B. G. Compton. Processing and mechanical characterization of short carbon fiber-reinforced epoxy composites for material extrusion additive manufacturing. *Compos Part B-Eng.* **2021**;223.

11.   S. Chandrasekaran, B. Yao, T. Y. Liu, W. Xiao, Y. Song, F. Qian, C. Zhu, E. B. Duoss, C. M. Spadaccini, Y. Li, M. A. Worsley. Direct ink writing of organic and carbon aerogels. *Mater Horiz.* **2018**;5(6):1166-1175.

12.   A. Sarmah, S. K. Desai, A. G. Crowley, G. C. Zolton, G. B. Tezel, E. M. Harkin, T. Q. Tran, K. Arole, M. J. Green. Additive manufacturing of nanotube-loaded thermosets via direct ink writing and radio-frequency heating and curing. *Carbon.* **2022**;200:307-316.

13.   M. G. Wimmer, B. G. Compton. Semi-solid epoxy feedstocks with high glass transition temperature for material extrusion additive manufacturing. *Addit Manuf.* 2022;54.

14.   S. K. Romberg, M. A. Islam, C. J. Hershey, M. DeVinney, C. E. Duty, V. Kunc, B. G. Compton. Linking thermoset ink rheology to the stability of 3D-printed structures. *Addit Manuf.* 2021;37.

15.   Q. Chen, L. Han, J. Ren, L. Rong, P. Cao, R. C. Advincula. 4D Printing via an Unconventional Fused Deposition Modeling Route to High-Performance Thermosets. *ACS Applied Materials & Interfaces.* 2020;12(44):50052-50060.

16.   J. B. Enns, J. K. Gillham. Time–temperature–transformation (TTT) cure diagram: Modeling the cure behavior of thermosets. *J Appl Polym Sci.* 1983;28(8):2567-2591.

17.   J. K. Wilt, D. Gilmer, S. Kim, B. G. Compton, T. Saito. Direct ink writing techniques for in situ gelation and solidification. *MRS Communications.* 2021;11(2):106-121.

18.   M. Ivankovic, L. Incarnato, J. M. Kenny, L. Nicolais. Curing kinetics and chemorheology of epoxy/anhydride system. 2003;90(11):3012-3019.

19.   M. R. Kamal, S. Sourour. Kinetics and thermal characterization of thermoset cure. 1973;13(1):59-64.

20.   M. G. B. Odom, C. B. Sweeney, D. Parviz, L. P. Sill, M. A. Saed, M. J. Green. Rapid curing and additive manufacturing of thermoset systems using scanning microwave heating of carbon nanotube/epoxy composites. *Carbon.* 2017;120:447-453.

21.   A. Sarmah, S. K. Desai, G. B. Tezel, A. Vashisth, M. M. Mustafa, K. Arole, A. G. Crowley, M. J. Green. Rapid Manufacturing via Selective Radio-Frequency Heating and Curing of Thermosetting Resins. *Adv Eng Mater.* 2022.

22.   A. Sarmah, A. Crowley, S. Desai, G. Zolton, M. J. Green. ADDITIVE MANUFACTURING OF THERMOSETTING RESINS VIA DIRECT INK WRITING AND RADIO FREQUENCY HEATING AND CURING. In: US Patent App. 18/072,190; 2023.

23.   M. Anas, M. M. Mustafa, A. Vashisth, E. Barnes, M. A. Saed, L. C. Moores, M. J. Green. Universal patterns of radio-frequency heating in nanomaterial-loaded structures. *Applied Materials Today.* 2021;23:101044.

24.   A. Vashisth, S. T. Upama, M. Anas, J. H. Oh, N. Patil, M. J. Green. Radio frequency heating and material processing using carbon susceptors. *Nanoscale Adv.* 2021;3(18):5255-5264.

25. T. Tarlton, E. Sullivan, J. Brown, P. A. Derosa. The role of agglomeration in the conductivity of carbon nanotube composites near percolation. *Journal of Applied Physics.* **2017**;121(8):085103.

26. M. V. C. Morais, A. I. Oliva-Avilés, M. A. S. Matos, V. L. Tagarielli, S. T. Pinho, C. Hübner, F. Henning. On the effect of electric field application during the curing process on the electrical conductivity of single-walled carbon nanotubes–epoxy composites. *Carbon.* **2019**;150:153-167.

27. A. Battisti, A. A. Skordos, I. K. Partridge. Dielectric monitoring of carbon nanotube network formation in curing thermosetting nanocomposites. *J Phys D Appl Phys.* **2009**;42(15).

28. A. de la Vega, J. Z. Kovacs, W. Bauhofer, K. Schulte. Combined Raman and dielectric spectroscopy on the curing behaviour and stress build up of carbon nanotube–epoxy composites. *Composites Science and Technology.* **2009**;69(10):1540-1546.

29. A. Sarmah, S. K. Desai, G. B. Tezel, A. Vashisth, M. M. Mustafa, K. Arole, A. G. Crowley, M. J. Green. Rapid Manufacturing via Selective Radio-Frequency Heating and Curing of Thermosetting Resins. *Adv Eng Mater.* **2022**;24(7).

30. A. Sarmah, M. A. Morales, A. Srivastava, S. Upama, A. Nandi, T. C. Henry, M. J. Green, A. Vashisth. Interfacial carbon fiber-matrix interactions in thermosetting composites volumetrically cured by electromagnetic fields. *Composites Part a-Applied Science and Manufacturing.* **2023**;164.

31. A. Vashisth, R. E. Healey, M. J. Pospisil, J. H. Oh, M. J. Green. Continuous processing of pre-pregs using radio frequency heating. *Compos Sci Technol.* **2020**;195.

32. M. L. Auad, S. R. Nutt, P. M. Stefani, M. I. Aranguren. Rheological study of the curing kinetics of epoxy–phenol novolac resin. **2006**;102(5):4430-4439.

33. A. Rusli, W. D. Cook, T. L. Schiller. Blends of epoxy resins and polyphenylene oxide as processing aids and toughening agents 2: Curing kinetics, rheology, structure and properties. **2014**;63(8):1414-1426.

34. L. S. Cividanes, W. Franceschi, F. V. Ferreira, B. R. C. Menezes, R. C. M. Sales, G. P. Thim. How Do CNT affect the branch and crosslink reactions in CNT-epoxy. *Materials Research Express.* **2017**;4(10).

35. S. A. Madbouly, J. U. Otaigbe. Kinetic Analysis of Fractal Gel Formation in Waterborne Polyurethane Dispersions Undergoing High Deformation Flows. *Macromolecules.* **2006**;39(12):4144-4151.

36. N. W. Radebe, C. Fengler, C. O. Klein, R. Figuli, M. Wilhelm. Rheo-IR: A combined setup for correlating chemical changes via FTIR spectroscopy and rheological properties in a strain-controlled rheometer. *J Rheol.* **2021**;65(4):681-693.

37. W. Du, L. Tan, Y. Zhang, H. Yang, H. Chen. Dynamic Rheological Investigation during Curing of a Thermoset Polythiourethane System. *International Journal of Polymer Science.* **2019**;2019:8452793.

38. P. Jyotishkumar, J. Pionteck, C. Özdilek, P. Moldenaers, U. Cvelbar, M. Mozetic, S. Thomas. Rheology and pressure–volume–temperature behavior of the thermoplastic poly(acrylonitrile-butadiene-styrene)-modified epoxy-DDS system during reaction induced phase separation. *Soft Matter.* **2011**;7(16):7248-7256.

39. C. Liu, L. Zheng, L. Yuan, Q. Guan, A. Gu, G. Liang. Origin of Increasing Dielectric Constant at Lower Percolation Threshold through Controlling Spatial Distribution of Carbon Nanotubes in Epoxy Resin with Microwave-Assisted Thermal Curing Technique. *The Journal of Physical Chemistry C.* **2016**;120(50):28875-28885.

40. Z. Leng, H. Wu, X. Tang, Y. Li, Y. Xin, P. Xie, G. Li, K. Yan, C. Liu. Carbon nanotube/epoxy composites with low percolation threshold and negative dielectric constant. *Journal of Materials Science: Materials in Electronics.* **2022**;33(34):26015-26024.

41. Z. Špitalský, S. N. Georga, C. A. Krontiras, C. Galiotis. Dielectric Spectroscopy and Tunability of Multi-Walled Carbon Nanotube / Epoxy Resin Composites. **2010**;19(6):096369351001900601.

42. Y. Yosida, I. Oguro. Variable range hopping conduction in multiwalled carbon nanotubes. *Journal of Applied Physics.* **1998**;83(9):4985-4987.